SAND2017-13158R

Sandia National Laboratories
Albuquerque, New Mexico 87185

*date:* November 27, 2017

*to:* D. VanGoethem

*from:* E. Corona

*subject:* MLEP-Fail Calibration for 1/8 inch thick plate of 13-8 PH steel in the H1150 condition

## Introduction

The purpose of the work presented in this memo was to calibrate the Sierra material model *Multilinear Elastic-Plastic Hardening Model with Failure*, (MLEP-Fail), for 1/8 inch thick plate of 13-8 PH steel in the H1150 condition. Material testing was pursued first, followed by the actual calibration. The material testing consisted of uniaxial tension tests on flat smooth and notched specimens. The notched specimens were manufactured with three notch radii: 1/8, 1/32 and 1/64 inches. The dimensions of the smooth and notched specimens are given in the prints in Appendix A. The calibration procedure had two steps. The first was to fit the multi-linear hardening function of the material to best match the measured engineering stress-strain responses. The second was to use the failure data from the smooth and notched specimens to calibrate the two parameters of the failure criterion in the model.

## Tensile Test Data

The tests were conducted at the Structural Mechanics Laboratory in New Mexico by Jhana Gearhart (1528) and Colin McConnell (1528) between August 31 and September 6, 2017. The work planning and control number of the testing activities is SML 4195. The basic properties listed in the MMPDS-08[1] are given in Table 1.

### Smooth Specimens

The smooth specimens were cut along three directions in the plate: along, transversely and at 45° to the rolling direction. All specimens were pulled to failure at two nominal strain rates: $0.73 \times 10^{-4}$ and $0.73 \times 10^{-3}$ $s^{-1}$ to explore possible rate dependencies that could affect

[1]Metallic Material Properties Development and Standardization, MMPDS-08, April 2013, Copyright Battelle Memorial Institution.

**Table 1.** Basic properties of 13-8 PH steel in the H1150 condition listed in the MMPDS-08

| Young's Modulus (Msi) | Poisson's Ratio | 0.2% Yield Stress (ksi) | Ultimate Stress (ksi) | Failure Strain |
|---|---|---|---|---|
| 28.3 | 0.28 | 90 | 135 | 0.14 |

the responses of the notched specimens. Figures 1 (a) through (c) show the engineering stress vs. strain curves obtained from the tests for each of the three specimen orientations. No significant effect of strain rate dependence is present in these tests. Figure 1(d) compares the curves with the minimum and maximum strain to failure ($\varepsilon_f$) from all directions. Little difference exists among all the curves prior to the ultimate stress. The spread afterwards is more significant, with the specimens at 45° seemingly having higher values of strain to failure.

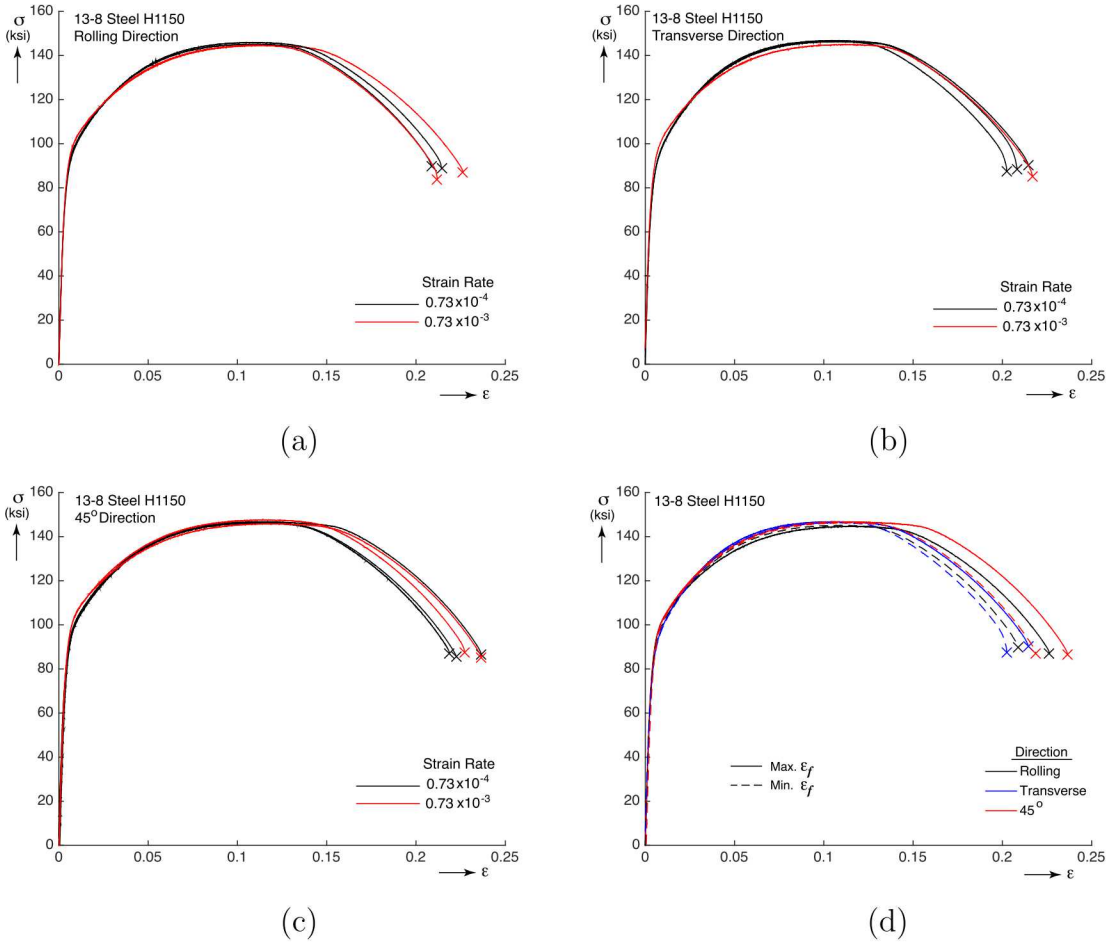


**Figure 1.** Measured engineering stress vs. strain curves. (a) Rolling direction, (b) transverse direction, (c) 45° direction and (d) comparison of curves with minimum and maximum engineering strain to failure for each direction.

### Notched Specimens

Two tests were conducted for each of the three notch radii with a displacement rate of $0.05 \times 10^{-3}$ inches per second. In each test, the axial displacement across the notch ($\Delta_L$) was measured with two extensometers, opposite to each other across the thickness. The gage lengths of the two extensometers ($L$) were one inch and 1/2 inches. Figure 2 shows the measured tensile load-deflection responses. The force $F$ has been normalized by the initial, nominal, minimun cross-sectional area in the notch ($A_o$). The results from the tests were nearly identical for each notch radius. As expected, as the notches get sharper, the displacement to failure decreases and the maximum load increases. In each case the displacements measured with the 1/2 inch extensometer were slightly smaller than those measured with the one inch extensometer.

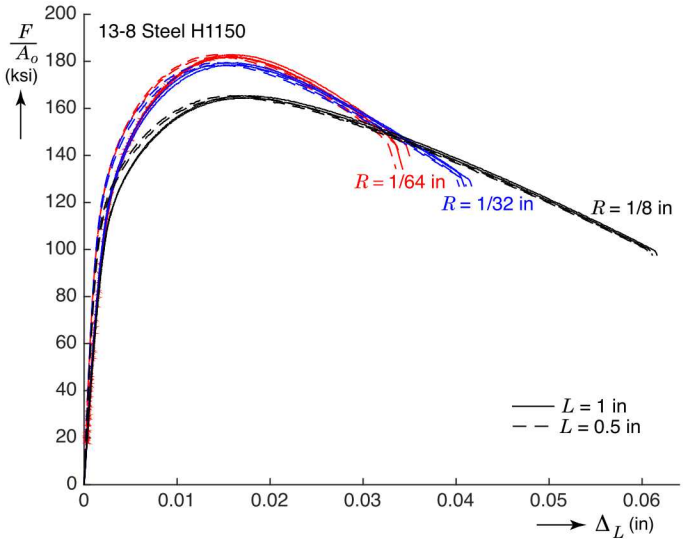


**Figure 2.** Measured load vs. deflection curves for tension tests of notched specimens with three notch radii. Tests were conducted in duplicate and each with two extensometers of gage lengths one and 0.5 inches.

## Calibration

### Hardening Function

The calibration of the hardening function requires an iterative process that determines the required hardening function to reproduce an experimentally measured engineering stress-strain curve. This was done using the script developed by Tim Shelton (1542), which utilizes an implicit quasi-statics finite element model of the specimen's gage length. The simulations used selective deviatoric elements. The form of the hardening function is multilinear. The curve chosen for calibration was along the rolling direction, with the minimum strain to failure and obtained at the faster strain rate (specimen R07 in Appendix B). The basic

properties of this curve are shown in Table 2. The value of Young's modulus was measured as the slope of the engineering stress-strain curve between 0.5 and 26 ksi. Appendix B shows the basic properties measured for all the tests on smooth specimens. Note that the properties listed in Tables 1 and 2 are very close, with the exception of the strain to failure, which was significantly higher in the specimens tested. Poisson's ratio was not measured in the tests, and the value listed in Table 2 was assumed prior to consulting the MMPDS-08.

It is well known that the determination of the hardening function can depend on the size of the element ($h_e$) if the specimen necks. Therefore, Figure 3 shows the results of the calibration using three models with element sizes of 0.02, 0.01 and 0.004 inches. Figure 3(a) shows the comparison between the measured and calculated engineering stress-strain responses. It shows very good agreement for most of the response. Only near the failure point the load calculated using the largest elements is a little high. The multi-linear hardening functions are shown in Fig. 3(b). The smaller the element, the higher the true stresses ($\sigma_t$) in the fit. This is as expected because using the smaller elements puts less constraint on the shape of the neck, thus allowing for a higher hardening function. The hardening function obtained with $h_e = 0.004$ in. was adopted for the calibration procedure of the failure criterion.

**Table 2.** Basic properties of fitted engineering stress-strain curve.

| Young's Modulus (Msi) | Poisson's Ratio [not measured] | 0.2% Yield Stress (ksi) | Ultimate Stress (ksi) | Failure Strain |
|---|---|---|---|---|
| 27.9 | 0.29 | 89.5 | 144.5 | 0.212 |

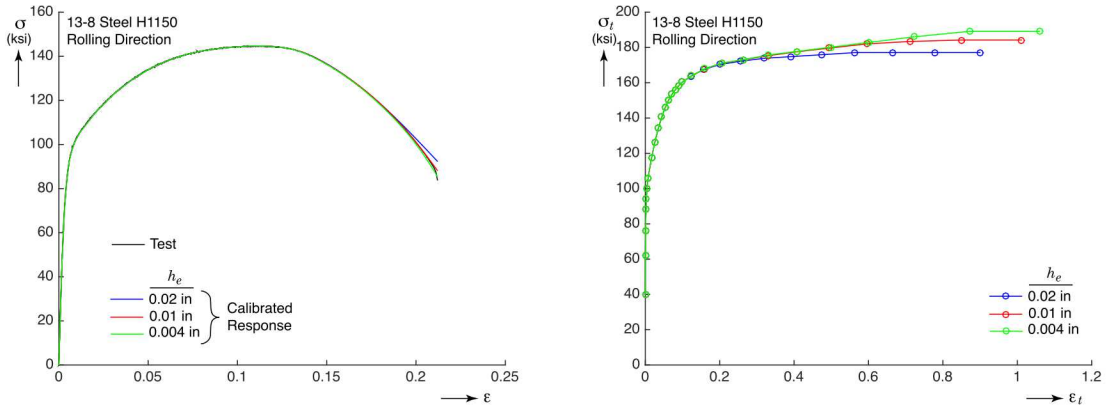


(a) (b)

**Figure 3.** Calibration of uniaxial tension test data as a function of element size. (a) Comparison of test and calibrated engineering stress vs. strain curves for a sample in the rolling direction and (b) required hardening curves.

**Failure Criterion**

The calibration of the failure criterion is based on data obtained from tension tests conducted on smooth and notched specimens. The first step is to simulate the notched tension tests using the hardening function obtained above. Figure 4 shows the results. Although some differences can be observed between the test and the simulation results, the predictions of the load vs. deflection responses are reasonably good. At this point no failure criterion has been used in the simulations, and they were continued beyond the end points shown in the figure.

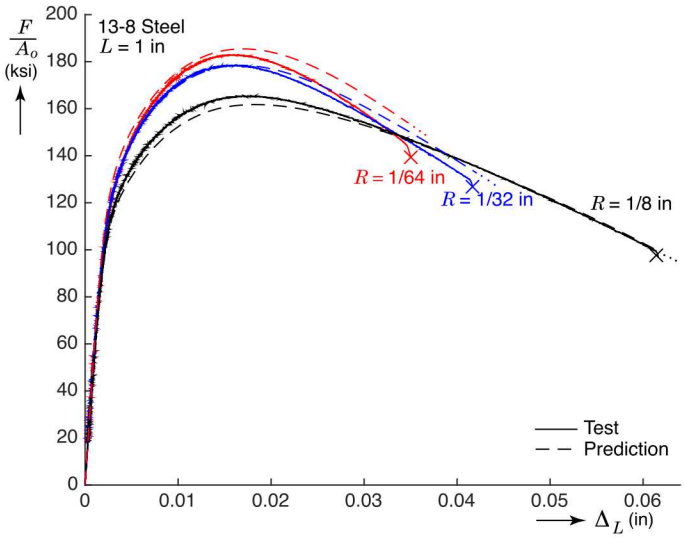


**Figure 4.** Comparison of measured and predicted responses for the tension tests on notched specimens.

The failure criterion in the MLEP-Fail model is commonly called *tearing parameter*. The criterion assumes that the material accumulates damage ($t_p$) according to

$$t_p = \int_0^{\varepsilon} \left\langle \frac{2\sigma_1}{3(\sigma_1 - \sigma_m)} \right\rangle^m d\varepsilon_p \tag{1}$$

where <> are Macaulay brackets, $\sigma_1$ and $\sigma_m$ are the maximum principal and mean hydrostatic stresses, and $d\varepsilon_p$ is an infinitesimal increment in equivalent plastic strain. The upper limit of integration represents the current value of equivalent plastic strain. The parameters of the model to be calibrated include the failure exponent, $m$ and the critical value of $t_p$ when material failure occurs, given by $t_p^{\text{crit}}$. The objective of the calibration procedure is to find appropriate values for $m$ and $t_p^{\text{crit}}$.

*Procedure*

The calibration procedure[2] consists of measuring the values of $\Delta_L^t$ in the tension tests at which failure occurred. The next step consists of running finite element models of the tension

[2]The calibration procedure is similar to that proposed in Reedlunn and Lu (2015), An Attempt to Cali-

tests on smooth and notched specimens and keeping a record of the values of $\sigma_1$, $\sigma_m$ and $\varepsilon_p$ at each solution step for the elements likely to be most critical. These elements are located in the narrowest part of the notches, or neck in the case of the smooth specimen. The selective deviatoric elements used have 8 integration points. In the calibration procedure, the average values of $\sigma_1$, $\sigma_m$ and $\varepsilon_p$ over the 8 integration points were used to calculate $t_p$. The models used initially all had elements with $h_e = 0.004$ inches[3]. Subsequently another calibration was conducted with elements of $h_e = 0.016$ inches. Once the simulations are done, the recorded values of $\sigma_1$, $\sigma_m$ and $\varepsilon_p$ can be used in a simple script to calculate $t_p$ at all critical elements, given a guess of $m$. The value of $t_p^{\text{crit}}$ can then be determined by trial and error by minimizing the difference between the values $\Delta_L^p$ calculated from the guessed values of the two parameters above and the corresponding measurements $\Delta_L^t$ from the tests. Here, the objective function to be minimized is

$$e = \sum_1^N \left| \frac{\Delta_L^p - \Delta_L^t}{\Delta_L^t} \right| . \tag{2}$$

where $N$ is the number of calibration tests considered, which is four in the present calibration.

*Results*

To set up the stage for the presentation of the results, the simple, traditional method of using a constant value of equivalent plastic strain based on the failure of a smooth uniaxial specimens will be considered first. Note that the constant equivalent plastic strain failure criterion is equivalent to the tearing parameter in (1) with $m = 0$. Figure 5(a) shows the result of applying this criterion to the simulation of the notched tension tests with element size of 0.004 in. This figure shows plots of the calculated load vs. deflection curves for all specimen geometries. The symbol $\times$ marks the displacement at which failure occurred in the tests while the symbol $\square$ represents the point at which failure would be predicted based on equivalent plastic strain. The two symbols necessarily coincide for the smooth specimen. From here, the critical value of equivalent plastic strain was $\bar{\varepsilon}_p = 1.4$. Note that the simulations overestimate the displacements at failure for all the notched tension tests. Figure 5(b) shows the same results when the element size was 0.016 in. In this case, $\bar{\varepsilon}_p = 0.95$, showing that ductile failure calibrations are element size dependent.

The effect of the element size on the predicted responses is shown in Fig. 6. The same hardening function obtained with $h_e = 0.004$ in. was used for both element sizes. Note that the calculated responses of the smooth specimen were identical up to the ultimate stress point but, as expected, diverged afterward. For the notched specimen simulations, the responses diverge earlier as the radius of the notch decreases.

Minimizing the objective function in (2) should give the optimum values of $m$ and $t_p^{\text{crit}}$ that best fits the test data. The procedure followed here consisted of fixing the value of $m$ to an

brate and Validate a Simple Ductile Failure Model Against Axial-Torsion Experiments on Al 6061-T651, SAND2015-20782

[3]Elements of this size gave reasonably well converged results for even the sharpest notch used here, as shown in a previous memo: Evaluation of Planar Notched Specimens for Failure Model Calibration, May 9, 2017.

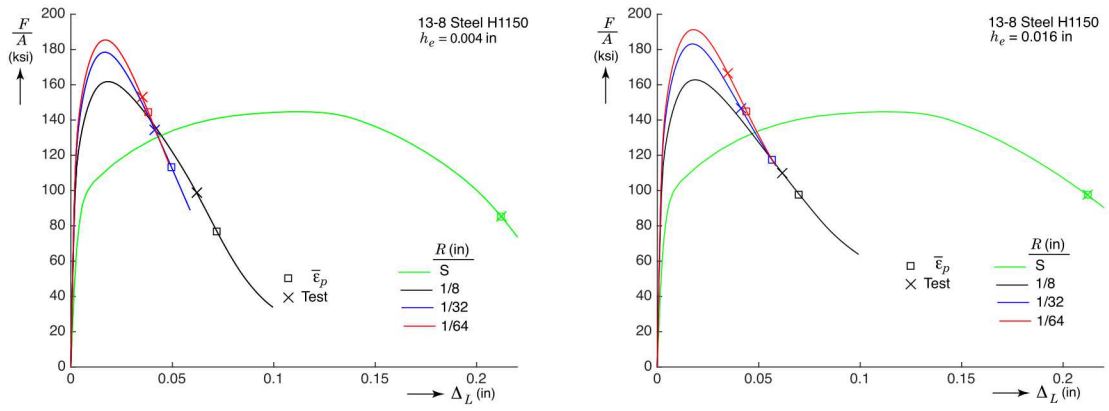


(a) (b)

**Figure 5.** Comparison of the failure points between test data and predictions by the constant equivalent plastic strain at failure criterion for two model element sizes when calibrated to match failure data in a uniaxial tension test. (a) $h_e = 0.004$ in. and (b) $h_e = 0.016$ in.

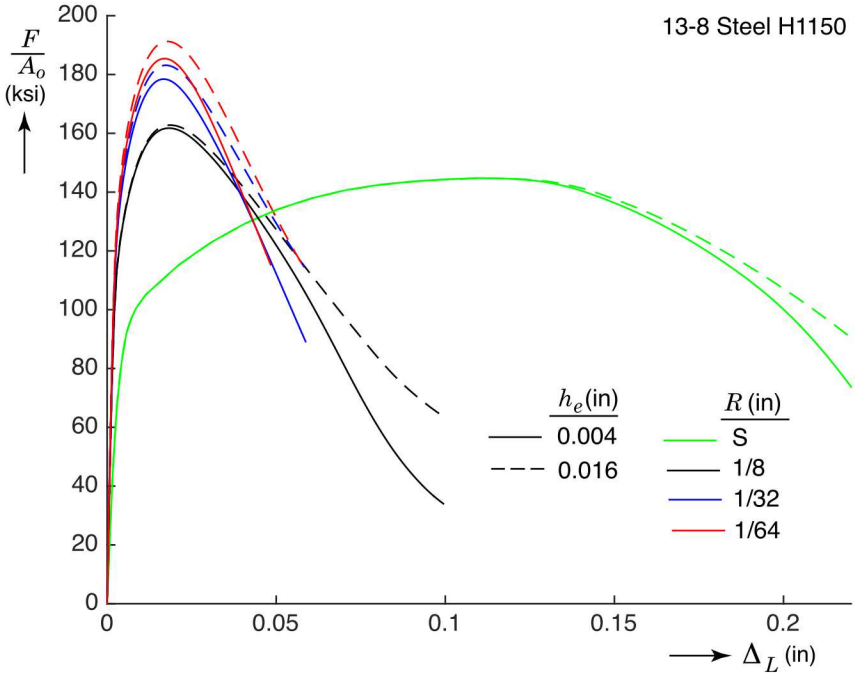


**Figure 6.** Comparison between load-deflection responses predicted with models of two element sizes. The same hardening function was used in both cases.

integer value and then finding the value of $t_p^{\text{crit}}$ that minimized the objective function. This value was found within $\pm 0.025$. The results are shown in Table 3 for both values of element size considered. Figure 7 shows the failure points marked on the predicted load-deflection responses for both element sizes used. Clearly the failure points are clustered around the test data and all fits are reasonable, which brings up the question: which one should be chosen? One approach is to pick the ones that gave the overall lowest value of the objective function. If this is the case then the best fits are $m = 4$ with $t_p^{\text{crit}} = 5.6$ and $m = 1$ with $t_p^{\text{crit}} = 1.1$ for $h_e = 0.004$ and 0.016 in., respectively. Actually when $h_e = 0.004$ in. the lowest value of the objective function occurred for $m = 5$, but the results presented were capped at $m = 4$ for reasons to be discussed next.

**Table 3.** Combinations of critical tearing parameter and failure exponent that fit the test data reasonably well for meshes with $h_e = 0.004$ and 0.015 inches.

| $h_e = 0.004$ in. | | $h_e = 0.015$ in. | |
|---|---|---|---|
| $m$ | $t_p^{\text{crit}}$ | $m$ | $t_p^{\text{crit}}$ |
| 0 | 1.15 | 0 | 0.75 |
| 1 | 1.60 | 1 | 1.10 |
| 2 | 2.05 | 2 | 1.50 |
| 3 | 3.35 | 3 | 2.15 |
| 4 | 5.60 | 4 | 3.05 |

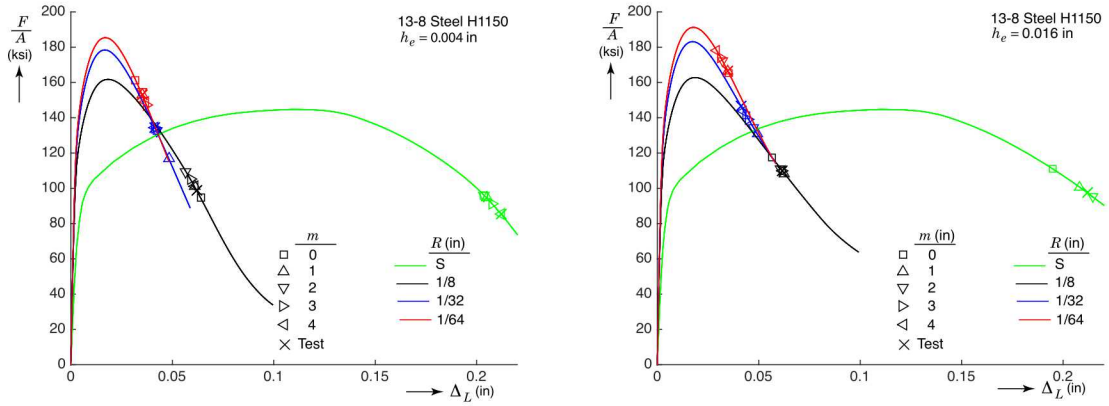


(a) (b)

**Figure 7.** Comparison of failure points for the calibrations presented in Table 3. (a) $h_e = 0.004$ in. and (b) $h_e = 0.016$ in.

The issue of which fit could be potentially more appropriate can not be categorically settled with the information that we have so far. This is even if we were to pustulate that the material fails exactly according to the tearing parameter, which is unlikely, and that the element size has no influence on failure, which is incorrect. Although the calculated failure points in Fig. 7 are clustered around the test data, there are significant differences in the failure details. For example, Fig. 8 shows the paths in plastic equivalent strain vs. triaxiality

($\varepsilon_p$ vs. $\eta$) space followed by the points where failure eventually occurred for two extreme cases, $m = 0$ and 4 with their respective values of $t_p^{\text{crit}}$. In the case with $m = 0$, shown in Fig. 8(a), the equivalent plastic strain to failure is independent of triaxiality, so all the calculated failure points lie along a horizontal. In this case, the smooth and notched specimen with $R = 1/8$ in. fail at the center of the notch while the specimens with $R = 1/32$ and $1/64$ fail at the edge of the specimen. The other case, when $m = 4$ as shown in Fig. 8(b) all failure points are at the center of the specimen, and the variation of equivalent plastic strain to failure with triaxiality is quite steep.

How flat or steep the variation of equivalent plastic strain is with triaxiality has significant implications on when failure would occur for states of stress that are have triaxialities that are not in the vicinity of the test data. For example, in the case of an ideal pure shear test, the triaxiality would be zero. The example shown in Appendix C shows that the expected strain to failure for zero triaxiality would range from $\bar{\varepsilon}_p = 1.15$ for $m = 0$ to $\bar{\varepsilon}_p = 28.3$ for $m = 4$. A factor of 20! A plastic strain to failure of 28.3 in pure shear seems unlikely, so the fits with, say, $m$ between 0 and 2 seem more likely. Note that the failure exponent does not have to be an integer as has been used here. A shear-dominated test to failure would greatly help improve the failure model calibration. Conversely at a triaxiality value of $\eta = 2$, the strain to failure could vary between 1.15 again for $m = 0$ and 0.07 for $m = 4$. Whereas current research is ongoing exploring the low triaxiality, or shear-dominated, regime, techniques for achieving high triaxialites in the order of 2 in the laboratory have not been investigated. Finally note that the range of triaxiality that the four tests in this work covered could vary significantly depending on what fit is considered. It could range from a relatively wide $0.4 < \eta < 1.1$ for the fit with $m = 0$ to a narrow $1.0 < \eta < 1.1$ for the fit with $m = 4$.

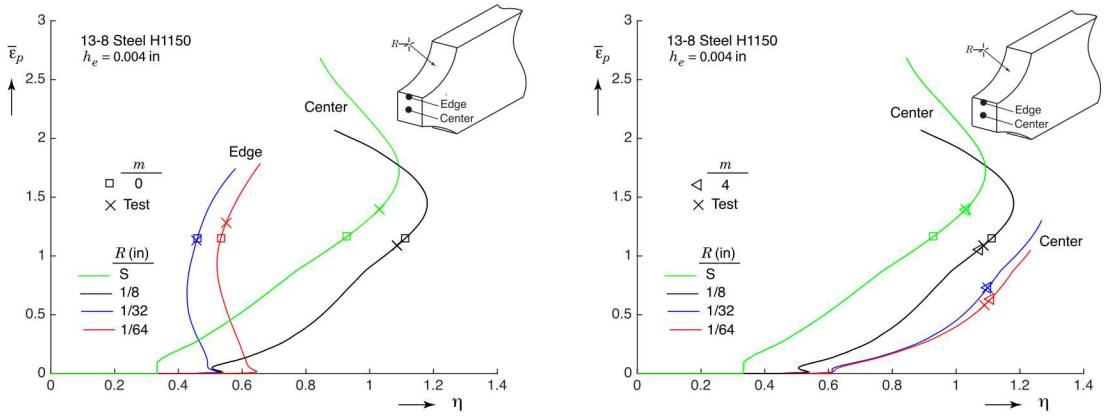


**Figure 8.** Paths in the equivalent plastic strain vs. triaxiality space for points where failure occurred and all specimen geometries considered. The failure points from test and calibration are shown. (a) $m = 0$ and (b) $m = 4$.

*Validation*

In order to validate the calibration procedure, the calibrations with $m = 2$ for both meshes

were used as input to the MLEP-Fail model in Sierra/SM. Simulations of all specimen geometries were then conducted, and the failure points as computed by Sierra/SM were compared against those that resulted from the calibration procedure. In most cases the difference in the displacements to failure as calculated with the calibration scripts and Sierra/SM was zero. Only when $R = 1/64$ in. was a difference of 3% detected. Although the reason for this difference has not been investigated, it is possible that it is due to the different order of operations used when averaging quantities over the element.

## Summary and Conclusions

This work concentrated on the calibration of Sierra/SM's MLEP-Fail model for 13-8 PH Steel in the H1150 condition. Multilinear forms of the hardening function were obtained employing the script developed by Tim Shelton for this purpose. The hardening function depends on the element size used in the finite element model of the uniaxial tension test. The curves obtained using the element sizes considered here were relatively close, but bigger elements could give rise to more substantial differences. Ideally, the smaller the element, the more representative the fit should become of the actual behavior, but it comes at the cost of increased computational time.

The calibration of the failure model (tearing parameter) was conducted based on failure data from smooth and notched tension specimens. The calibration of the failure model was not unique given the data available. The reason for the non-uniqueness was discussed, and it boils down to having insufficient data. The solution to this issue is to obtain other failure points that are removed from the range of triaxialities achieved in these tests. A possible test is a low-triaxiality, shear dominated test. The feasibility and utility of such tests are currently being investigated. Another possibility that may be useful to remove some of the uncertainty that gave rise to the non-unique calibrations is based on the data in Fig. 8 by determining the location where failure initiated in the specimens. It may be possible to image the fracture surfaces using an SEM to find the region where failure initiated, but there are no guarantees that the observations will be successful.

The calibration of the failure criterion also depends on the element size used to model the specimens. This is an important observation because the combination of geometry and element size used in applications can significantly influence the predicted loads at failure, as has been shown in many previous studies.

In conclusion, a recommendation for the use of the failure criterion would be to use the fits with $m \leq 2$, while being mindful of the element size used in the applications. Obviously this does not put us in a state where the model can be accurate in predicting ductile failure. Given that demands for failure prediction by computational means will continue, gahtering experience in the area will in time improve our abilities to deliver more credible failure assessments.

## Acknoledgments

Thanks go to the staff in the Structural Mechanics Laboratory in Org. 1528. Jhana Gorman and Colin McConnell conducted the material testing. Jack Heister produced the specimen drawings and coordinated the manufacture of the samples.

*Sandia National Laboratories is a multimission laboratory managed and operated by National Technology and Engineering Solutions of Sandia, LLC, a wholly owned subsidiary of Honeywell International, Inc., for the U.S. Department of Energy's National Nuclear Security Administration under contract DE-NA0003525.*

## Appendix A: Specimen Prints

Figures 9 and 10 show the manufacturing prints of the specimens used.

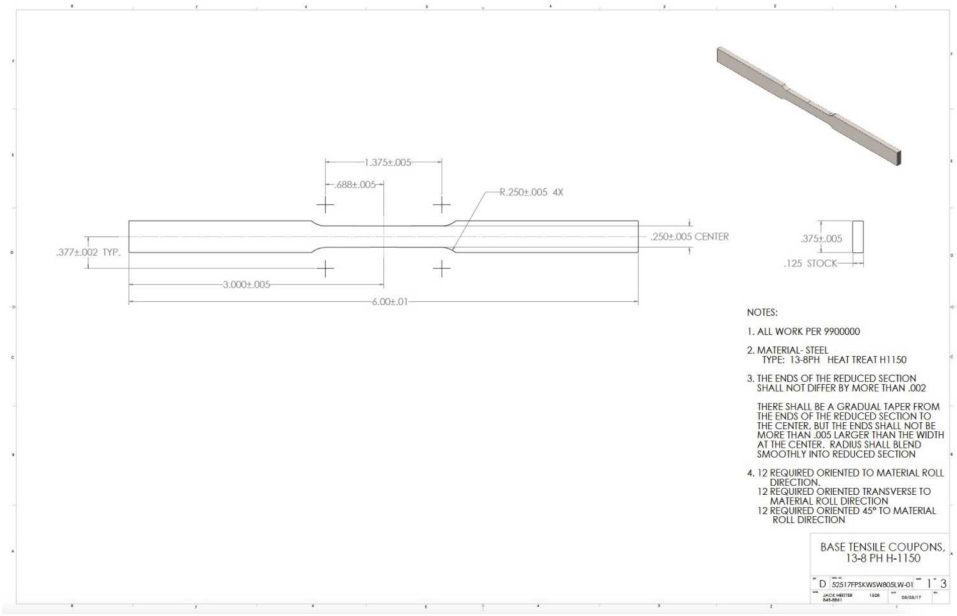


**Figure 9.** Smooth specimen.

## Appendix B: Material Properties Measured at the SML

Table 4 presents the values of the basic material properties measured at the Structural Mechanics Laboratory. The R and T labels indicate whether the specimen axis was along the rolling or transverse directions of the plate, while the 45 label indicates the axis of the specimen was at 45° to the rolling direction. The letter F indicates the faster strain rate. The Young's modulus was measured as the slope of the stress-strain curve in the range between one and five ksi. Specimen R07 was used to conduct the fit of the hardening function.

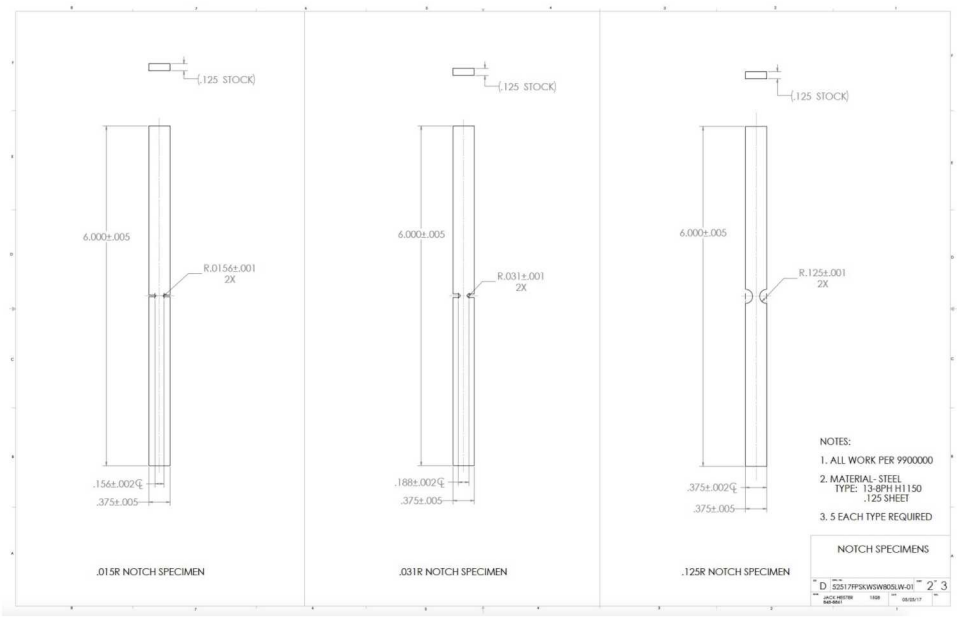


**Figure 10.** Notched specimens.

**Table 4.** Basic material properties measured from all smooth specimens in the Structural Mechanics Laboratory.

| Specimen | Young's Modulus (Msi) | 0.2% Yield Stress (ksi) | Ultimate Stress (ksi ) | Failure Strain |
|---|---|---|---|---|
| R05 (F) | 29.4 | 88.3 | 145.0 | 0.226 |
| R06 | 29.4 | 84.3 | 146.3 | 0.214 |
| R07 (F) | 28.0 | 89.7 | 145.0 | 0.212 |
| R10 | 28.1 | 87.8 | 145.7 | 0.209 |
| T01 | 29.5 | 87.4 | 145.4 | 0.217 |
| T03 | 29.3 | 83.4 | 147.0 | 0.215 |
| T09 | 28.5 | 83.9 | 147.1 | 0.208 |
| T10 (F) | 28.7 | 82.3 | 146.9 | 0.203 |
| 45-2 (F) | 29.0 | 91.6 | 148.0 | 0.227 |
| 45-4 | 30.1 | 84.3 | 146.2 | 0.223 |
| 45-6 | 29.1 | 87.5 | 147.3 | 0.237 |
| 45-7 | 28.5 | 87.9 | 146.4 | 0.219 |
| 45-12 (F) | 28.8 | 91.6 | 146.3 | 0.237 |

## Appendix C: Example of the Dependence of Equivalent Plastic Strain at Failure on Triaxiality for MLEP-Fail Model

To illustrate an example of the relation between the equivalent plastic strain to failure and triaxiality, consider a state of stress given by:

$$\boldsymbol{\sigma} = \begin{bmatrix} \sigma_H & \tau & 0 \\ \tau & \sigma_H & 0 \\ 0 & 0 & \sigma_H \end{bmatrix}. \tag{3}$$

The principal stresses are given by:

$$\sigma_1 = \sigma_H + \tau,\ \sigma_2 = \sigma_H,\ \sigma_3 = \sigma_H - \tau, \tag{4}$$

and, assuming a $J_2$ or von Mises yield function, the equivalent stress is given by

$$\sigma_e = \sqrt{3}\tau. \tag{5}$$

The triaxiality is defined as the ratio of the mean hydrostatic stress to the equivalent stress and is given by

$$\eta = \frac{\sigma_m}{\sigma_e} = \frac{\sigma_H}{\sqrt{3}\tau}. \tag{6}$$

Substituting the values of $\sigma_m$ and $\sigma_1$ into (1) gives the following relation

$$t_p = \left[\frac{2}{3}\left(\sqrt{3}\eta + 1\right)\right]^m \varepsilon_p. \tag{7}$$

Finally, solving for $\varepsilon_p$ in terms of $t_p$ and considering failure gives

$$\bar{\varepsilon}_p = \left[\frac{2}{3}\left(\sqrt{3}\eta + 1\right)\right]^{-m} t_p^{\text{crit}}. \tag{8}$$

Plots of (8) are shown in Fig. 11(a). Fig. 11(b) shows a close-up for lower values of $\bar{\varepsilon}_p$. Note that increaing the value of $m$ makes the curves steeper,thus giving higher values of $\bar{\varepsilon}_p$ for low $\eta$ and lower for high $\eta$.

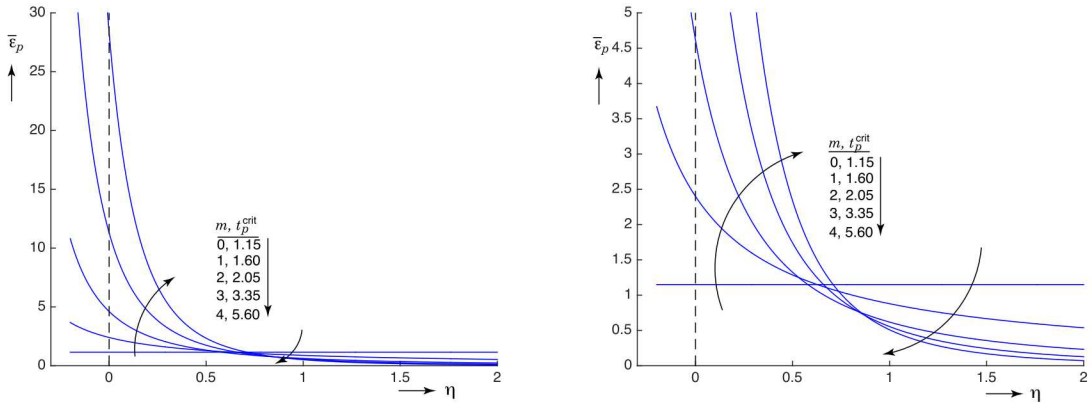


**Figure 11.** Equivalent plastic strain at failure vs. triaxiality plots for the example problem and the $(m,t_p^{\text{crit}})$ combinations in Table 3 for $h_e = 0.004$.

**Internal Distribution:**

| | |
|---|---|
| J. Gearhart | 1528 |
| M. Guthrie | 1553 |
| E. Fang | 1554 |
| B. Lester | 1554 |
| B. Reedlunn | 1554 |
| W. Scherzinger | 1554 |
| D. VanGoethem | 1554 |
| J. Ostien | 8343 |